Environmental Security Technology Certification Program

ESTCP

Blossom Point Marine Transect Survey Statistical Analysis with Visual Sample Plan.

ESTCP Project # 200325

Final Report
5/12/2008

B. Roberts,[1] J. Hathaway,[2] S. McKenna,[1] B. Pulsipher[2]
Sandia National Laboratories[1]
Pacific Northwest National Laboratory[2]

Distribution Statement A: Approved for Public Release, Distribution is Unlimited

Contents

1. Introduction 1
2. Transect Survey Performed 1
3. Transect Survey Data Analysis 2
   3.1. High Anomaly Density Area Flagging Parameters – Window Size 2
   3.2. High Anomaly Density Area Flagging Parameters – Critical Density 8
   3.3. Geostatistical Density Mapping 11
   3.4. High Density Area Delineation 14
4. Conclusions 17
5. References 18
Appendix A Results from Studies Using 500-m and 100-m Window Diameters 1

List of Figures

Figure 1. The traversed transects (black lines) and identified anomalies (blue points) for the Blossom Point marine survey. 2
Figure 2. Depiction of the window density calculation process used to identify high-density regions within a site. 3
Figure 3. Example of different window sizes, and how they would encompass the transect lines. 4
Figure 4. Flagged high-density regions from an 800-m diameter window using a 5-ApA critical density (top), and the histogram of site densities with a red line marking 5 ApA (bottom). 5
Figure 5. Flagged high-density regions from a 350-m diameter window using an 8-ApA critical density (top), and the histogram of site densities with a red line marking 8 ApA (bottom). 6
Figure 6. Flagged high-density regions from a 240-m diameter window using a 10-ApA critical density (top), and the histogram of site densities with a red line marking 10 ApA (bottom). 7
Figure 7. Overlaid flags using a 10-ApA critical density with a 240-m window diameter (orange) and a critical density of 8 ApA with a 350-m window diameter (purple). The boundary of the 800-m window diameter flags from a 5 ApA critical density also is shown (green). 8
Figure 8. Histogram of 350-m window densities with frequency plotted on the y-axis (top) and a log distorted frequency y-axis (bottom). Both figures use the 8 ApA critical density. 9
Figure 9. The Blossom Point site with three different displayed critical densities. The 9 ApA critical density (green) is the top layer with the 8 ApA layer (red) below and the 7 ApA layer (purple) at the bottom. 10
Figure 10. Final flagged regions determined using the VSP software with 350-m window and a critical density of 8 ApA. 10
Figure 11. Variogram for the Blossom Point study area. Black dots represent empirical data; the green line represents the functional model fit to the empirical data points. 12
Figure 12. Anomaly density values (ApA) for the Blossom Point study area. Areas without anomaly density color shading were not estimated because observational data were not available. 13
Figure 13. Portion of survey area for which digital bathymetric data were not available. For reference, color-coded anomaly density estimates and survey transect locations also are shown. 14
Figure 14. Cumulative distribution of estimated anomaly density values for the Blossom Point study area. 15
Figure 15. Delineation of highly impacted areas based on anomaly density values. Areas with anomaly densities greater than 8 ApA are shaded in red. 15

List of Tables

Table 1. Statistics for the kriging estimates of anomaly density developed for the Blossom Point study area. 13
Table 2. Anomaly count distribution by depth for those areas where digital bathymetric data were available. 13
Table 3. Anomaly count distribution by depth for those areas with estimated anomaly densities above 8 ApA and for which digital bathymetric data were available. 16

1. Introduction

The Environmental Security Technology Certification Program (ESTCP) has been evaluating several site characterization technologies for unexploded ordinance (UXO) site characterization. One of those ESTCP sponsored technologies developed by PNNL and SNL includes statistical algorithms that use the data quality objective structure to create appropriate sparsely spaced transect designs and then analyze these surveyed transects to identify potential target areas within the surveyed area. These transect design and mapping tools provide a statistically defensible method that uses transect survey data from a small proportion of the total study area (i.e., 1 to 3 percent) to identify target areas of a specific size, shape, and anomaly density.

Target area density estimates, target probability estimates, and density flagging routines are applied after the surveys are performed to separate potential target areas from areas that require no further remediation. These methods have been deployed within the Visual Sample Plan (VSP) software tool.

Evaluations and demonstrations of several integrated land-based characterization technologies have been documented in reports about previous Wide Area Assessment demonstration sites in Colorado, Ohio, and California (Roberts et al. 2007; Hathaway et al. 2006, 2007, 2008). In addition, ESTCP has been evaluating and demonstrating underwater site characterization technologies. One demonstration involved an underwater site along the Potomac River adjacent to the U.S. Army's Blossom Point Field Test Facility in Maryland. An underwater geophysical transect survey was designed and conducted by the ESTCP team and contractor. The PNNL/SNL team was then asked to use the target area flagging, anomaly density mapping and estimation, and target area delineation tools within the VSP software to perform an analysis of the survey results.

This report documents the application of these statistically based site characterization tools for the marine transect survey conducted at the U.S. Army's Blossom Point Field Test Facility in Maryland. These tools are used to 1) identify high anomaly density regions along the transects, 2) estimate anomaly densities across the site using the transect anomaly density data, and 3) delineate areas likely impacted by former munitions use at the site. Because munitions use at the Blossom Point facility primarily involved testing (USACE 2007), it is not known if actual target points were used within the firing fans. For this reason, this analysis focused on identifying areas impacted by former munitions use rather than actual target areas.

2. Transect Survey Performed

The transect survey was designed and conducted by the ESTCP sponsored project team previous to involvement in the project by PNNL and SNL. All associated analyses of the archive search report and conceptual site models were performed by that project team and the firing fans identified in Figure 1 were provided. The transect survey design placed transects 125-m apart and employed 5-m wide marine survey equipment for deeper

waters and 2-m wide shallow water skiff survey equipment. This survey traversed 328 line-km (204 mi) and covered 3.56 percent of the 4154-ha (10,266-ac) site.

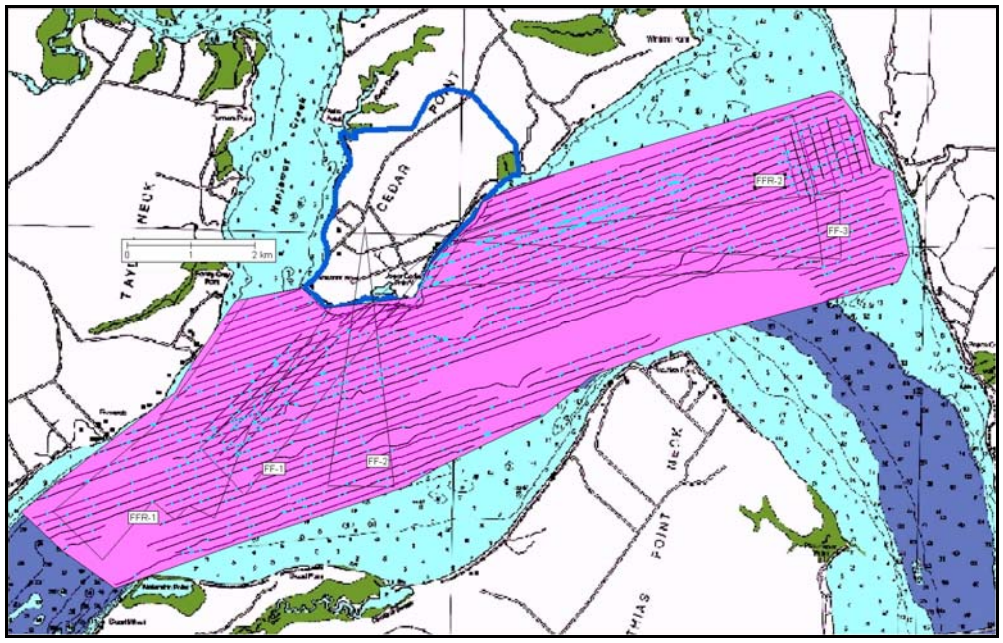

Figure 1. The traversed transects (black lines) and identified anomalies (blue points) for the Blossom Point marine survey.

3. Transect Survey Data Analysis

The anomaly locations and actual transect course data were provided to the PNNL/SNL team. Several iterative analyses were performed using the VSP high anomaly density area flagging tools to establish appropriate flagging and geostatistical parameters. Next the VSP geostatistical evaluation methods were employed to map and estimate the anomaly densities within flagged impact areas. These results are summarized within this section.

3.1. High Anomaly Density Area Flagging Parameters – Window Size

The first step in the process of identifying areas where the anomaly density is unusually high is to define the anomaly density along the transects. To identify high-density areas along transects, the Visual Sample Plan (VSP) software passes a window over segments of the site and calculates the anomaly density for each segment. The window diameter specifies the size of the circular area over which the average density is computed. Figure 3 shows how the window diameter is used to calculate transect grid densities. The window diameter defines the size of a circular window (orange and blue circles in Figure 2), which moves one-sixth of the selected diameter and uses the anomaly count and the transect area within it to calculate a density. This density is assigned to the transect grid (orange and blue boxes in (Figure 2) centered in the window. The green dots in Figure 2

represent the identified anomalies within the two surveyed transects. This figure provides an example of two of the multiple transect grid densities that would be calculated based on these transects.

The selection of an appropriate window diameter is dependent on the size of the target area of interest, transect width, and spacing between transects. The optimum window diameter is one that has sufficient traversed area within the window without including such a large area that potential high-density areas can be masked by the surrounding low-density areas in the window. The blue window in Figure 3 provides an example of a window that is too large (the orange area represents a potential target area). If the window diameter is too small (red window in Figure 3), then the limited amount of traversed area within the window is not sufficient to make accurate transect grid density estimates and usually results in “fliers” or isolated flags in different regions of the site. Within these two extremes, there are often many different window diameters that would be appropriate. Generally, the window diameter should be less than the diameter of the target area of interest and no smaller than the spacing between the original transect design.

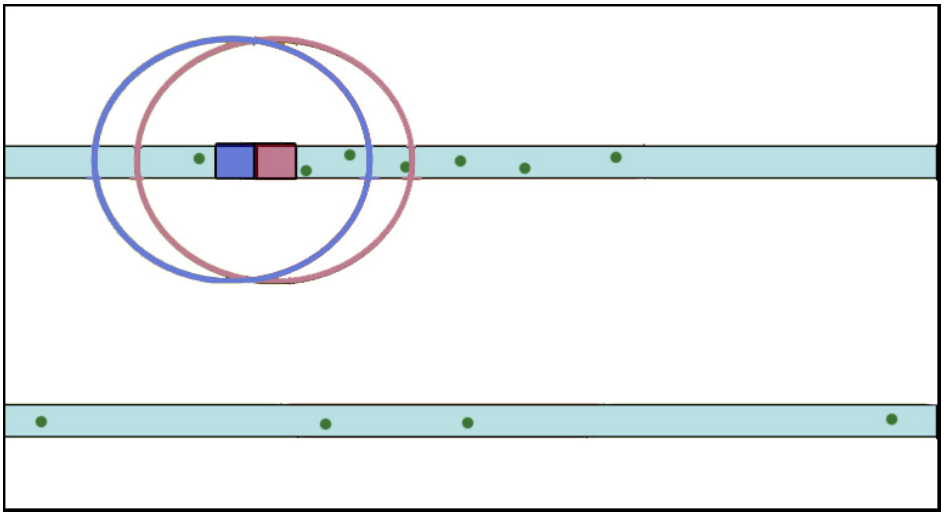

Figure 2. Depiction of the window density calculation process used to identify high-density regions within a site.

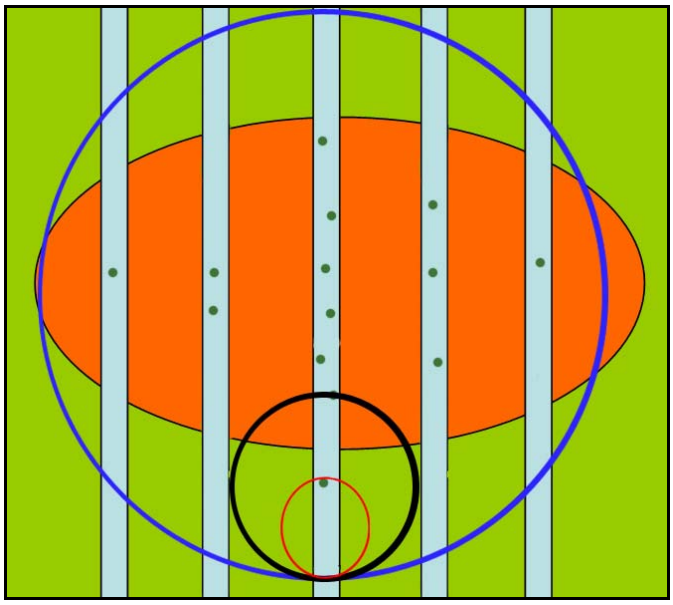

Figure 3. Example of different window sizes, and how they would encompass the transect lines.

While it is difficult to display the entire procedure used to select an appropriate window diameter, this section demonstrates some of the different window diameters that were examined for this Blossom Point analysis. Figures 4 through 6 provide three different examples of window diameter (800-m, 350-m, and 240-m) and critical density combinations examined to identify the optimal window diameter. The critical densities for the resulting flagged regions of high density in each figure were optimized using the histogram shown with each figure. Figure 7 shows the overlaid flagged regions from Figure 5 (350-m window) and Figure 6 (240-m window) and the boundary of the flagged regions from Figure 4 (800-m window). Additional figures displaying results from two other window diameters (i.e., 500 m and 100 m) are provided in the appendix. For a detailed description of the process of selecting the optimal window size, see Hathaway et al. (2008).

Using an 800-m diameter window created the anomaly density per acre (ApA) histogram shown in Figure 4. The critical density of 5 ApA resulted in the flagged regions shown above the histogram. The regions identified with this critical density and window diameter are generally the same regions as those in Figure 5 (350-m window). While the general location of the higher density areas within the site can still be distinguished from the background, this large window with a critical density of 5 ApA creates large boundaries around each of these locations. These large boundaries compared to the other window diameters also can be seen in Figure 7.

At the other extreme, there is no clear critical density for the 240-m window diameter that identifies the general high-density areas without many additional isolated flagged locations located over the site. The critical density of 10 ApA labeled in the histogram shown in Figure 6 is slightly higher than would typically be chosen based on the histogram alone; however, the flagged regions shown above the histogram are dispersed

throughout the site. The results from this window diameter demonstrate that any window diameter less than 240 m is too small and produces counter-intuitive results.

The 350-m window diameter used to produce the results shown in Figure 5 is determined to provide an appropriate window diameter. This window diameter did not flag many isolated high-density areas like the 240-m window. In addition, except for two isolated flagged locations, all of the flagged regions from the 350-m diameter window fell within those regions identified with the 800-m window but the large area averaging effect observed with the 800-m window results was eliminated. **Thus, the 350-m window diameter is recommended and used for the subsequent analyses described in this report.**

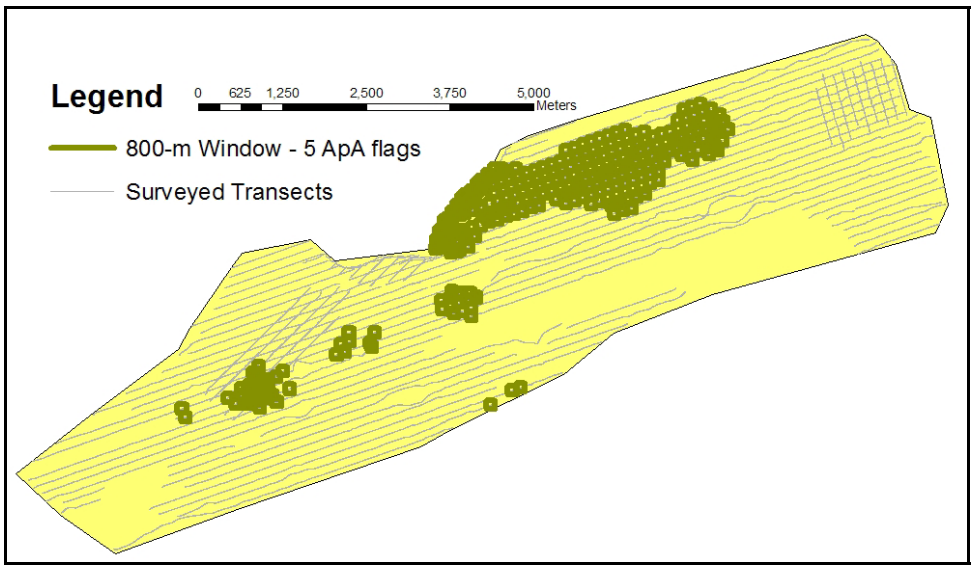

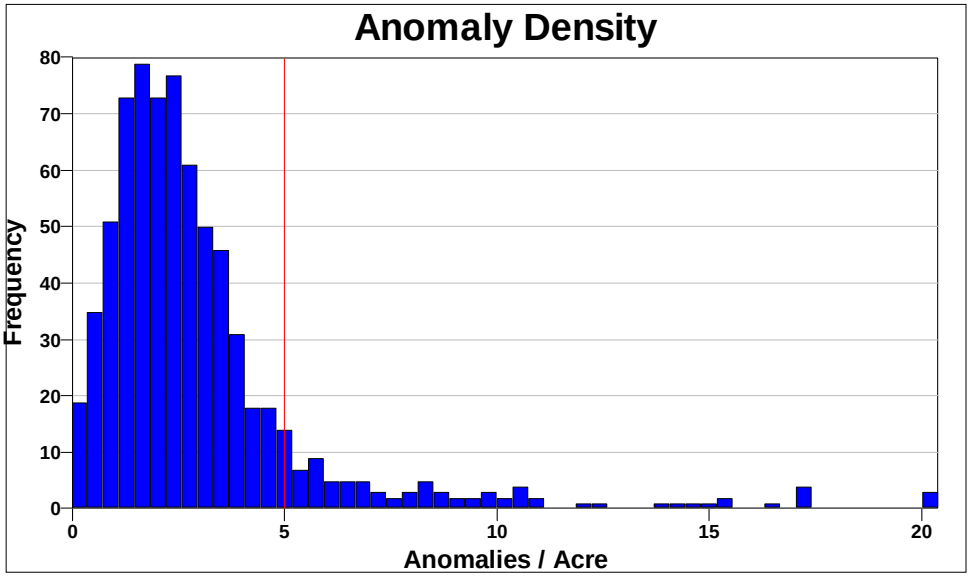

Figure 4. Flagged high-density regions from an 800-m diameter window using a 5-ApA critical density (top), and the histogram of site densities with a red line marking 5 ApA (bottom).

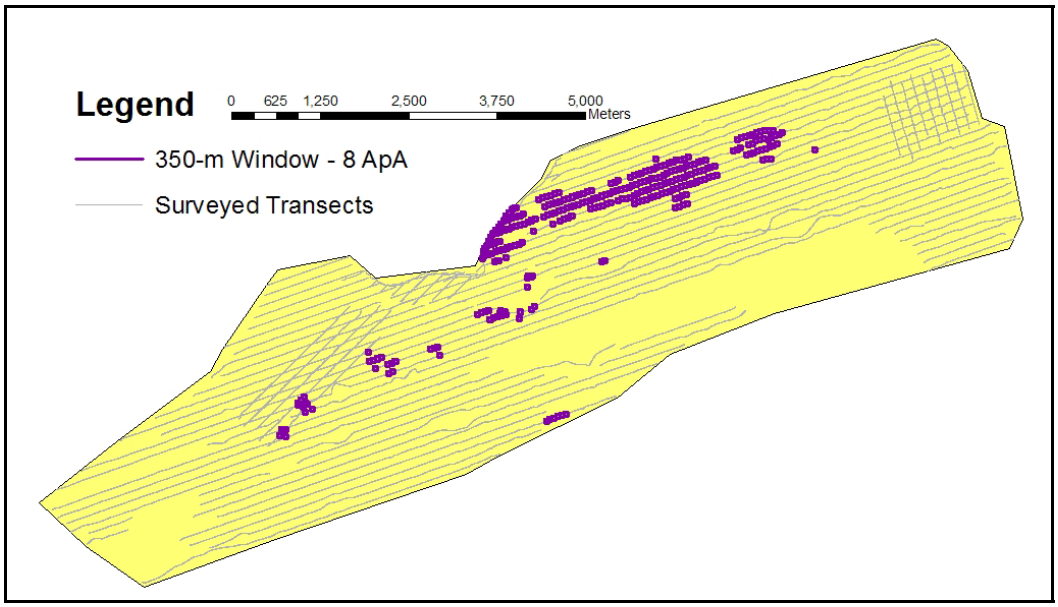

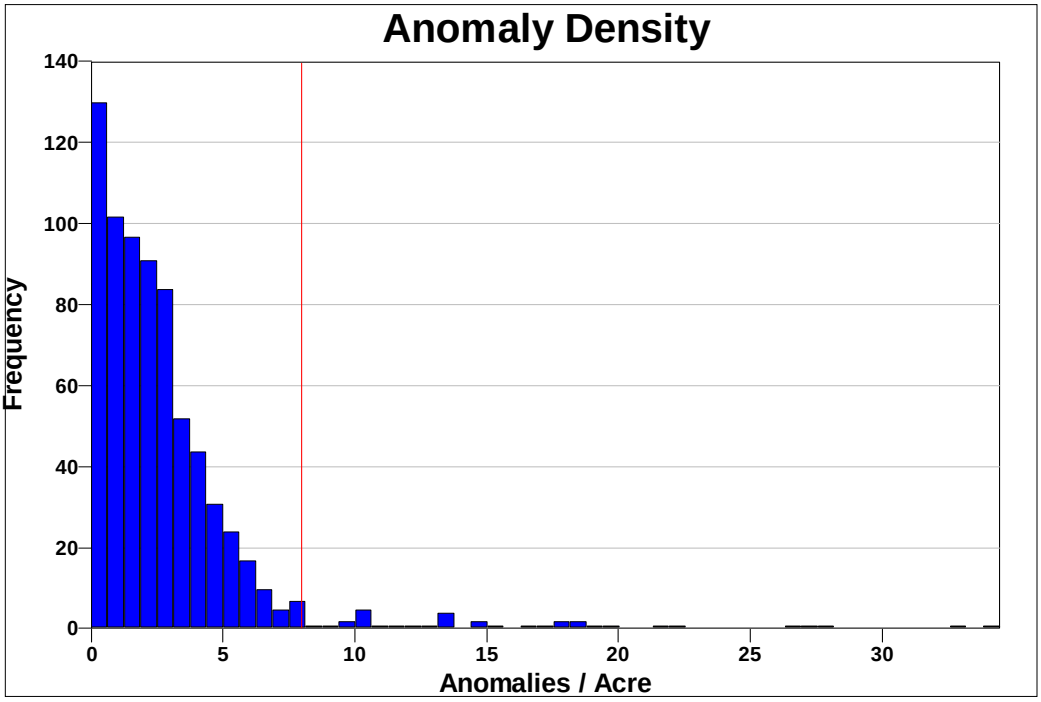

Figure 5. Flagged high-density regions from a 350-m diameter window using an 8-ApA critical density (top), and the histogram of site densities with a red line marking 8 ApA (bottom).

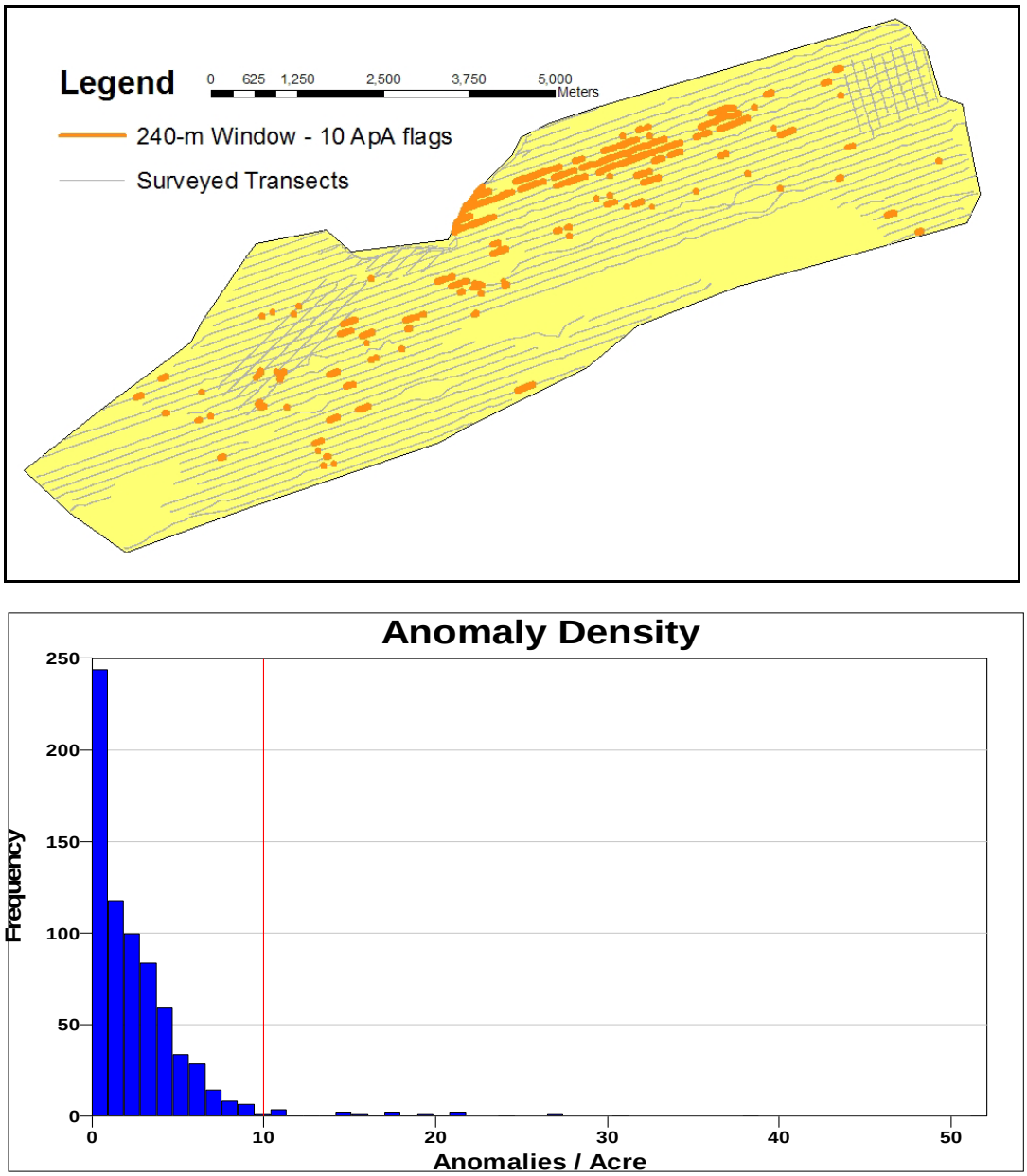

Figure 6. Flagged high-density regions from a 240-m diameter window using a 10-ApA critical density (top), and the histogram of site densities with a red line marking 10 ApA (bottom).

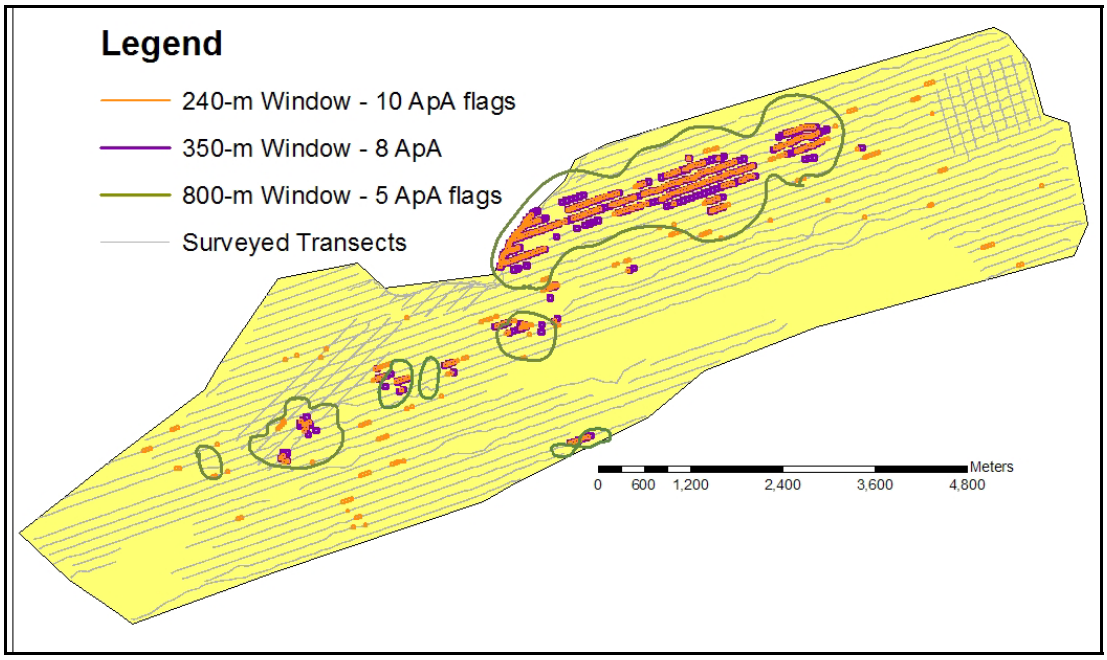

Figure 7. Overlaid flags using a 10-ApA critical density with a 240-m window diameter (orange) and a critical density of 8 ApA with a 350-m window diameter (purple). The boundary of the 800-m window diameter flags from a 5 ApA critical density also is shown (green).

3.2. High Anomaly Density Area Flagging Parameters – Critical Density

After the averaging window diameter is determined in the VSP flagging routine, the critical density, another important parameter, must be selected. The process of determining the appropriate critical density for Blossom Point is shown in this section. Figure 8 shows two histograms of the anomaly densities from the Blossom Point site as calculated using the 350-m diameter window. The upper histogram has frequency on the y-axis, and the lower histogram is displayed with a log transformed y-axis. From Figure 8, the tail of the distribution of background densities appears to transition to anomaly density values derived from high-density regions somewhere between 7 and 9 ApA.

Figure 9 shows the resulting flagged regions from three different critical densities (7, 8, and 9 ApA). This figure is overlaid to mask the lower critical densities with the higher critical densities. This display of the flagged regions from three different critical densities was the final tool used to select the appropriate critical density.

From Figure 9, the critical density of 7 ApA shows the beginning of isolated flags appearing throughout the site, and all critical densities below 7 ApA produce many more isolated flags. The flags from the larger critical density of 9 ApA (green) begin to miss the grouped flagged regions identified with the 8 ApA critical density. In addition, the boundary of the larger contiguous flagged region in the northern portion of the site does not change significantly with any of the three displayed critical densities. The final selection of 8 ApA reduces the number of isolated flags without significantly reducing

the boundary of the identified high-density regions. Figure 10 shows the final flagged regions from VSP using a 350-m window diameter and a critical density of 8 ApA.

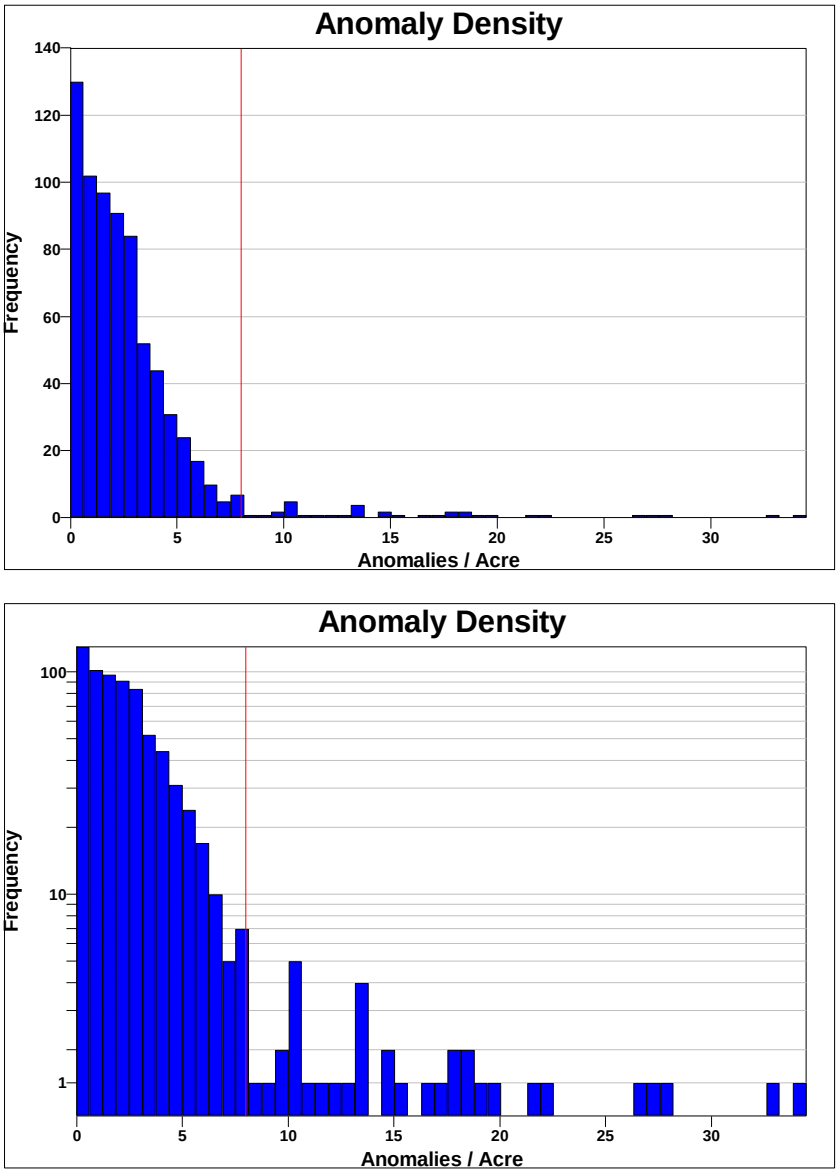

Figure 8. Histogram of 350-m window densities with frequency plotted on the y-axis (top) and a log distorted frequency y-axis (bottom). Both figures use the 8 ApA critical density.

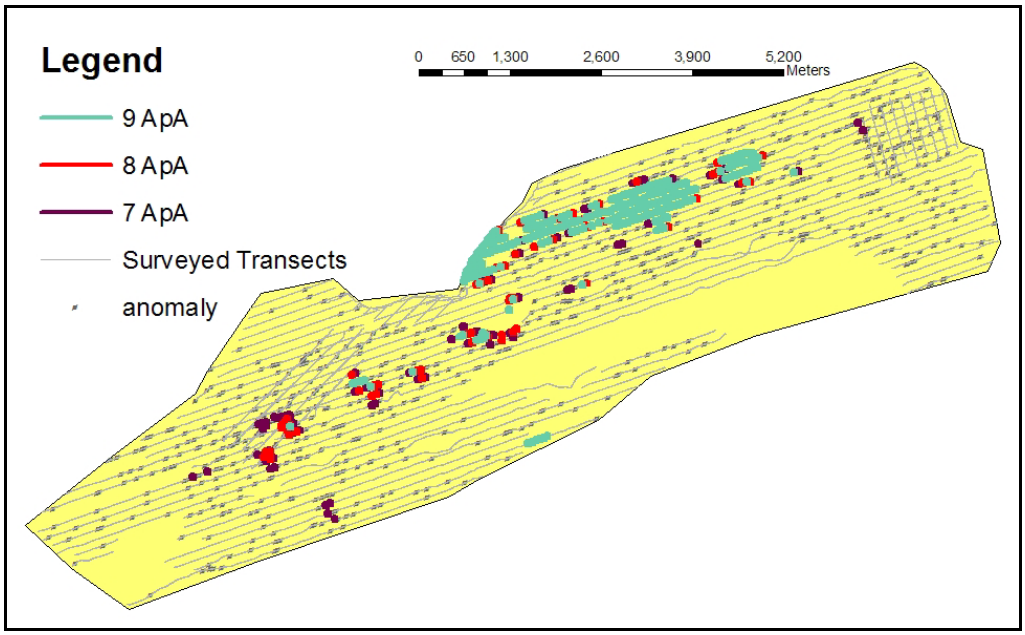

Figure 9. The Blossom Point site with three different displayed critical densities. The 9 ApA critical density (green) is the top layer with the 8 ApA layer (red) below and the 7 ApA layer (purple) at the bottom.

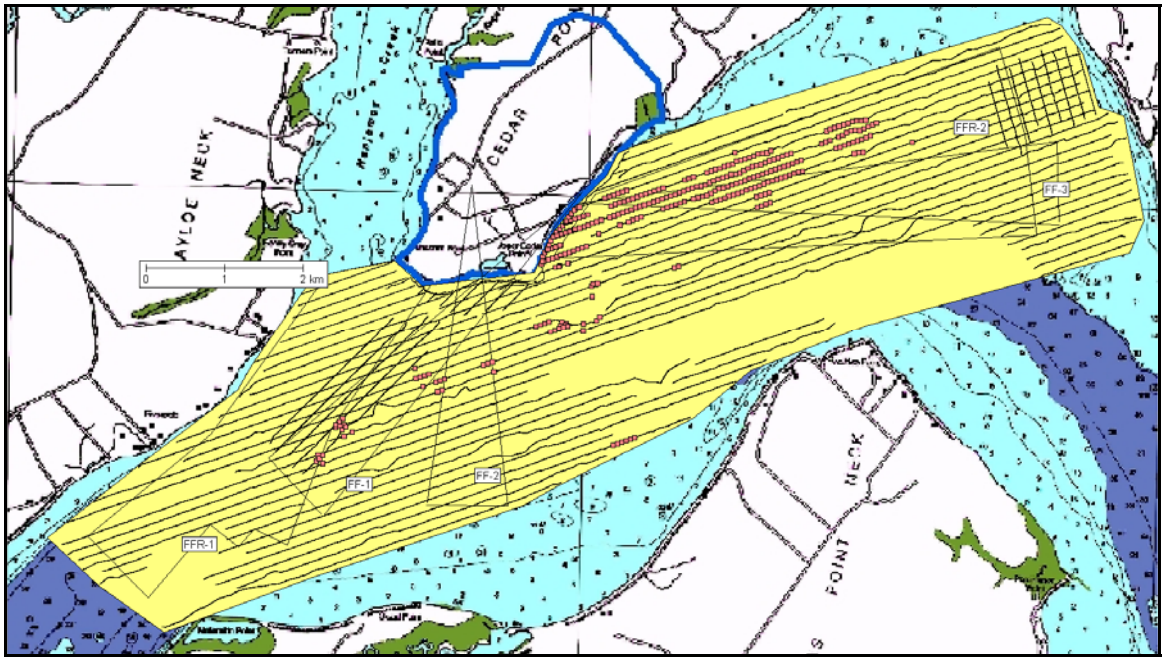

Figure 10. Final flagged regions determined using the VSP software with 350-m window and a critical density of 8 ApA.

3.3. Geostatistical Density Mapping

To assist in the delineation of high anomaly density areas, geostatistical (kriging) estimates of anomaly density were developed using the sample transect data. The geostatistical estimates provide values of anomaly density at unsampled areas away from the survey data transects and, therefore, provide a more comprehensive depiction of anomaly density patterns across the study area. This comprehensive depiction is valuable in the selection of high-density areas that may represent areas impacted by former munitions use as well as for target boundary delineation and estimation of the total number of anomalies at the site.

The geostatistical analyses were conducted using the VSP software package. The same magnetic anomaly location and course-over-ground data used in other VSP analyses presented in this report were also used directly in the geostatistical analyses. In addition, the same averaging window (350 m) used in previous sections of this report was adopted for all the geostatistical analyses.

All the transect and anomaly data from the study area, including all 5-m and 2-m transects, were combined and used as a single sample data set for the geostatistical analysis. The transect-based anomaly density values were computed from the anomaly location data and the transect survey area using a 350-m averaging window. It is these transect-based anomaly density data that were then used in the geostatistical analysis.

The initial step in the geostatistical analysis was the development of the variogram model. The spatial structure of the transect-based anomaly density data was investigated using an empirical variogram. This calculation creates a series of points that depict how the variability of the transect-based anomaly density data changes with increasing distances between the observational data. With most spatially dependent data sets, the typical situation is for the variability to increase with increasing distance between observations.

As shown in Figure 11, the empirical variogram from this data conforms with the expectation that variability will increase with increasing separation distance. Figure 11 shows the empirical variogram values (black dots) and the functional model fit to those data (green line). The variogram model was manually fit to the empirical data using a single function. This functional model then was used directly by the kriging estimator in the development of the estimates of anomaly density.

The kriging estimator within the VSP software package generates estimates for a grid of points covering the area of interest. For the estimates considered here, a grid with an equal spacing of 25 m for both the X and Y directions was used. This grid was oriented so that the X direction and Y direction were parallel to the east-west and north-south geographic directions, respectively. The kriging estimates were conditioned to the available observational data; that is to say, the estimates at unsampled locations were based on weighted averages of the surrounding observational data, and all observed density values are reproduced exactly in the kriged estimates. A maximum search radius for the inclusion of observational data was set to increase computational efficiency and to

maintain the effect of local variations in the observational data. A maximum search radius of 350 m was used in the kriging of the Blossom Point study site. Although, the use of the 350-m search radius did maintain the integrity of local features, it did result in some limited areas having insufficient data for estimation. If the kriging estimator did not have sufficient data for generating an estimate, that location was flagged as being "unestimated." This result is desirable to the extent that it prevents the generation of estimates for regions that are far from any observational data.

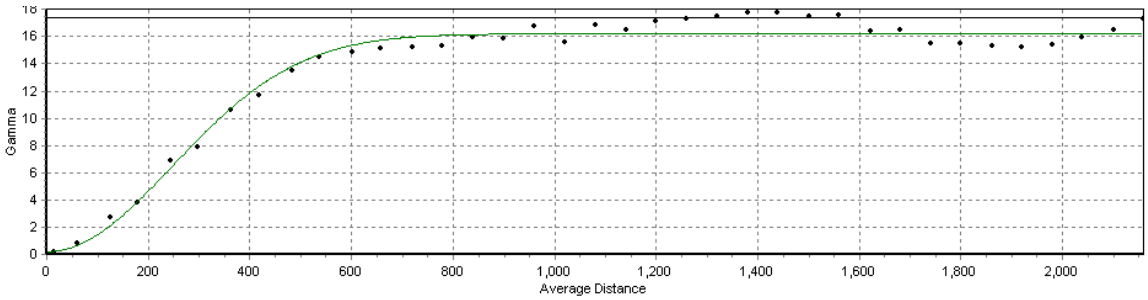

Figure 11. Variogram for the Blossom Point study area. Black dots represent empirical data; the green line represents the functional model fit to the empirical data points.

Figure 12 shows the estimated anomaly density developed by the kriging of the transect sample data. In this figure, the anomaly density values are denoted by color shading for those areas where sample transect data were available. The sample transect locations are identified by gray lines. A majority of the study area has anomaly density values of less than 8 ApA, but there are several distinct locations with anomaly density values significantly above this level. The most prominent high-density area occurs in the north-central portion of the study area. This area has density values approaching 40 ApA, with the high-density values forming an elongate form that starts at the shoreline and extends in a northeast direction. Several higher density zones are situated within this elongate area. In addition, there are several isolated high-density areas located near the center of the study area. These areas are smaller in size, have lower density values, and not as continuous as the larger high-density area. Basic statistics summarizing the anomaly density estimates shown in Figure 12 are provided in Table 1.

In addition, Table 2 lists the distribution of estimated magnetic anomaly counts based on bathymetric depth. The bathymetry data used to generate this listing is from a 1962 survey (NOAA 1962). This data was available for a majority of the surveyed area, exclusive of a portion of the surveys along the eastern border of the survey area. The values listed in Table 2 are only for those areas for which digital bathymetric data was available.

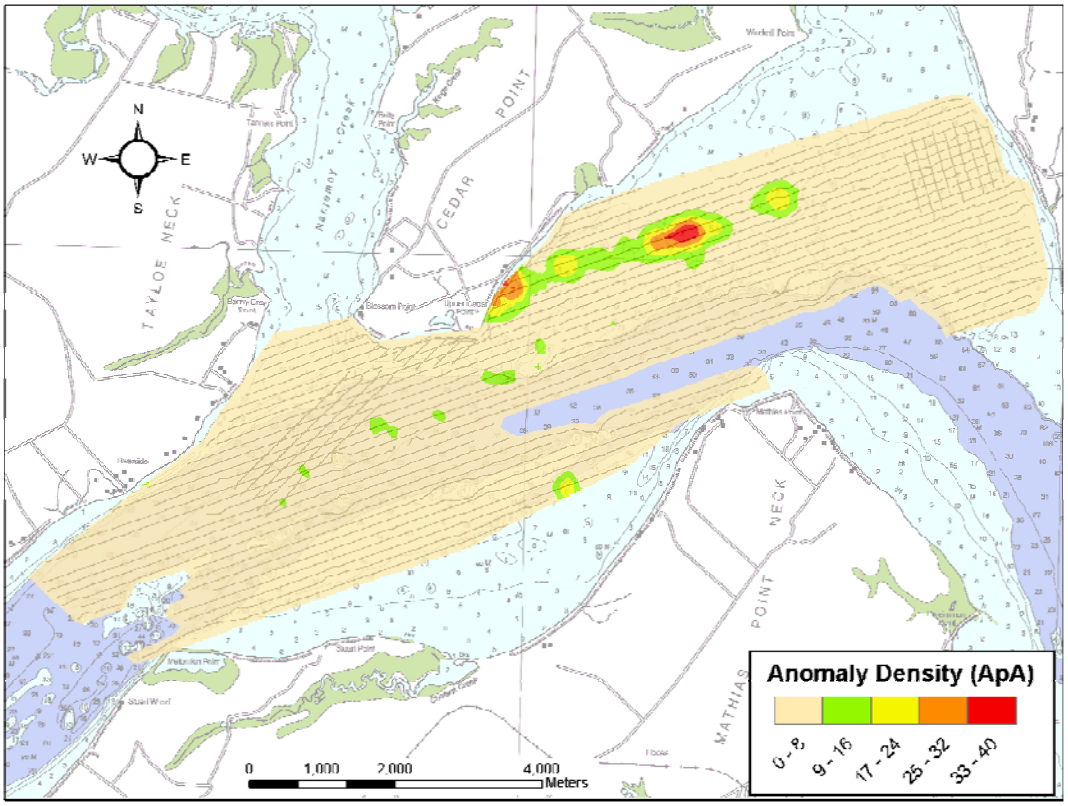

Figure 12. Anomaly density values (ApA) for the Blossom Point study area. Areas without anomaly density color shading were not estimated because observational data were not available.

Table 1. Statistics for the kriging estimates of anomaly density developed for the Blossom Point study area.

Statistic	Value
Total Area (ac)	9,310
Total Anomaly Count	27,954
Minimum Anomaly Density (ApA)	0.0
1st Quartile (ApA)	0.9
Mean Anomaly Density (ApA)	3.0
3rd Quartile (ApA)	3.7
Maximum Anomaly Density (ApA)	39.2

Table 2. Anomaly count distribution by depth for those areas where digital bathymetric data were available.

Depth (m)	Total Area (ac)	Total Anomaly Count
0 - 5	5,557	17,218
5 - 10	3,384	8,820
10 -20	482	366
> 20	37	2

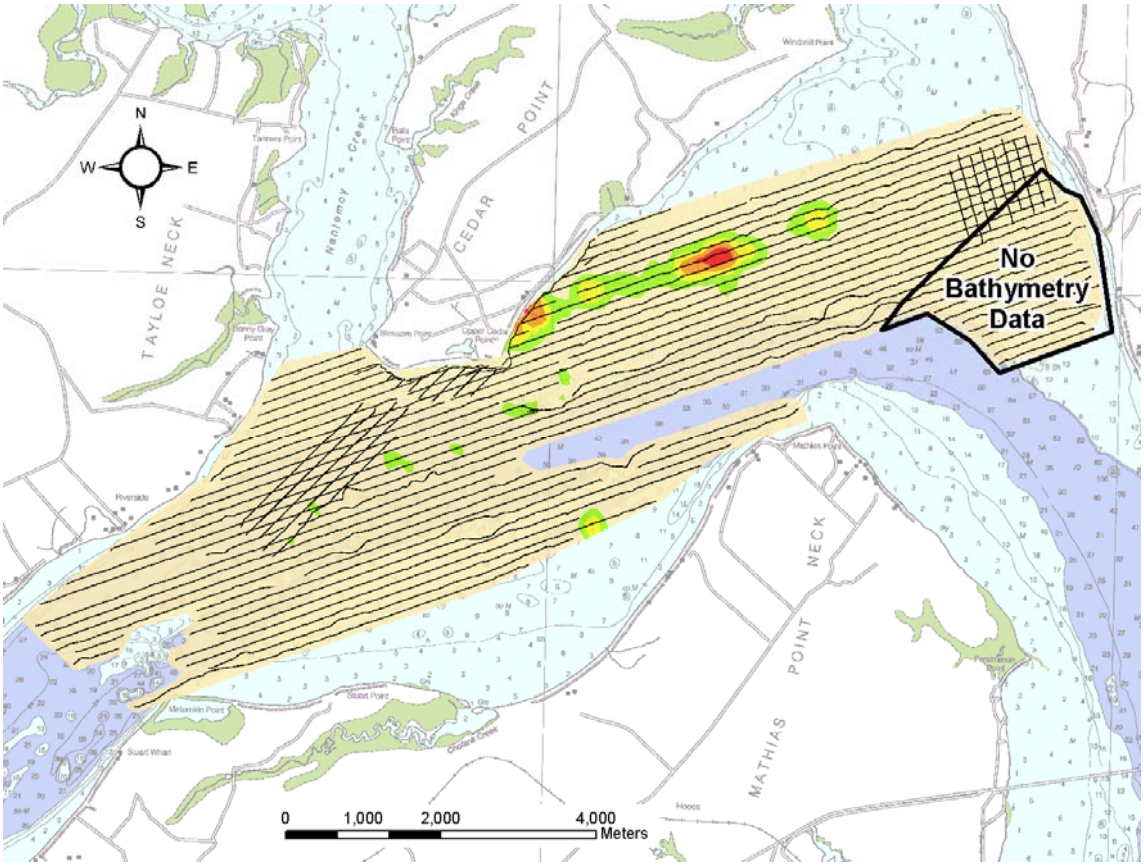

Figure 13. Portion of survey area for which digital bathymetric data were not available. For reference, color-coded anomaly density estimates and survey transect locations also are shown.

3.4. High Density Area Delineation

As discussed previously (Section 3.2), the transition from background anomaly densities to anomaly densities representing areas impacted by former munitions use appears to take place at densities somewhere between 7 and 9 ApA. Figure 14 shows the cumulative distribution of estimated anomaly density values for the Blossom Point study area. The break in slope of the cumulative curve confirms that the transition from background to impacted areas to be somewhere in the 7 to 9 ApA area.

Similar to the VSP flagging analysis presented in Section 3.2, an intermediate value of 8 ApA will be adopted for the delineation of likely impacted areas for the Blossom Point study area.

Figure 15 shows the locations at the Blossom Point study site with anomaly densities above 8 ApA shaded in red. The total area shaded in red comprises approximately 513 ac and includes an estimated total of 7900 magnetic anomalies. Table 3 gives the anomaly count distribution by depth for those areas above the 8 ApA threshold level.

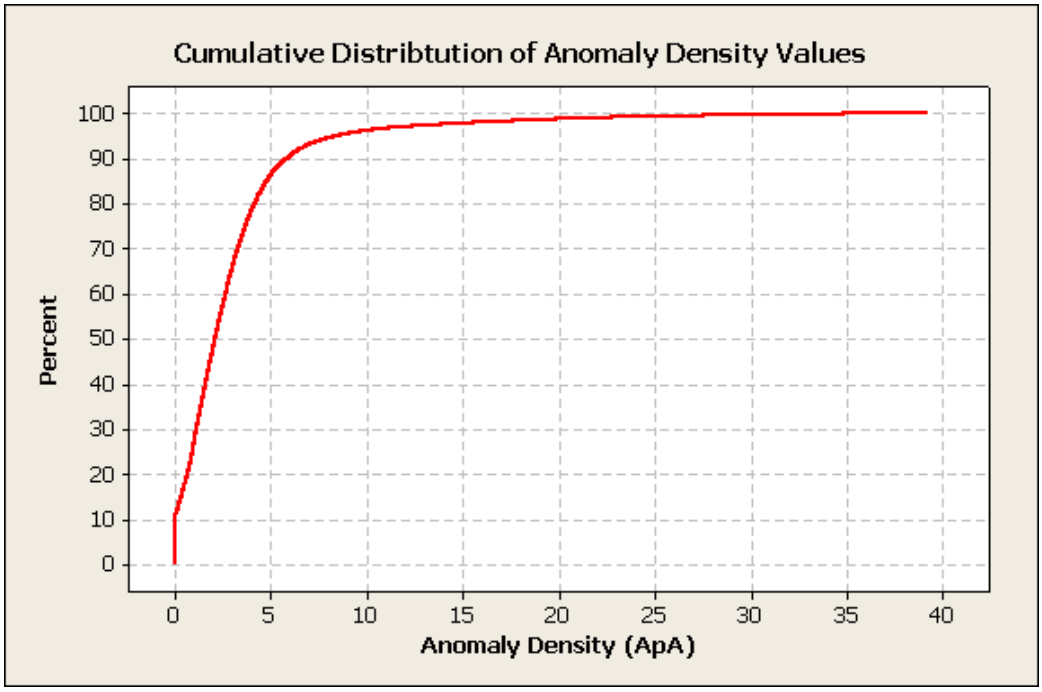

Figure 14. Cumulative distribution of estimated anomaly density values for the Blossom Point study area.

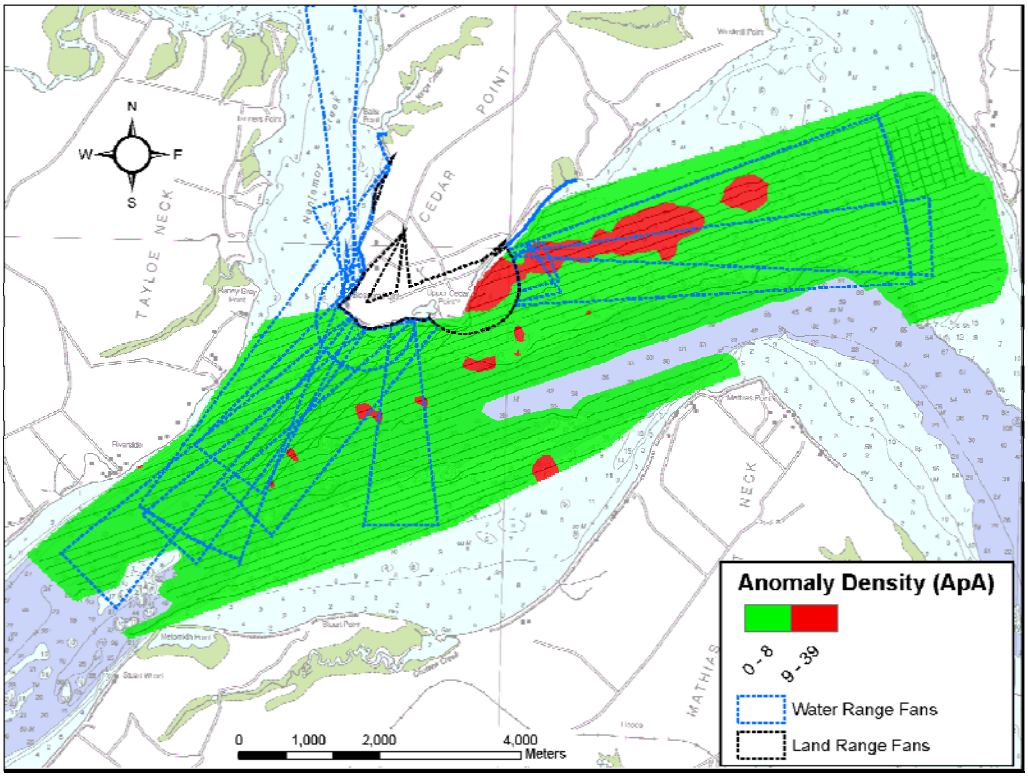

Figure 15. Delineation of highly impacted areas based on anomaly density values. Areas with anomaly densities greater than 8 ApA are shaded in red.

Table 3. Anomaly count distribution by depth for those areas with estimated anomaly densities above 8 ApA and for which digital bathymetric data were available.

Depth (m)	Total Area (ac)	Total Anomaly Count
0 – 5	462	7,419
5 – 10	52	500
10 – 20	0	0
> 20	0	0

The blue and black dotted lines in Figure 15 denote former water and land firing range fans, respectively, for the Blossom Point study area. As shown in this figure, the largest anomaly density mass that exceeds 8 ApA (in the northeastern portion of study area) corresponds to and is parallel to several water range firing fans. In addition, the region directly adjacent to the shoreline corresponds to the extent of a land firing range. The other identified areas in the study site with anomalies greater than 8 ApA are less massive and have only limited correlation to the known firing fans.

4. Conclusions

This report has presented analyses based on a sub-aqueous magnetometer survey of the area around the Blossom Point Field Test Facility along the Potomac River in Maryland. Statistical investigation of the magnetic anomaly density value distributions and the spatial patterns of the magnetic density values suggest that a threshold value of 8 ApA would be appropriate for delineating areas exhibiting significant impact from munitions use at the site.

Using a delineation threshold of 8 ApA, a total of 513 ac of the Blossom Point study area show sufficiently high anomaly density values as to be considered significantly impacted by munitions use at the Blossom Point facility. There are an estimated 7900 geophysical anomalies within this high-density area. A majority of this area is composed of a single, elongate concentration of magnetic anomalies located in the northeastern portion of the study area. The other areas with anomaly densities greater than 8 ApA consists of smaller isolated patches scattered around the study area. The larger anomaly concentration shows a close correspondence to documented firing fans. Although there is some overlap between the smaller anomaly concentrations and the documented firing fans, this correspondence is weaker, and in some cases, the anomaly concentrations do not correspond to any documented firing fans.

5. References

Hathaway J, BL Roberts, SA McKenna, and BA Pulsipher. 2006. *Application of Statistically-Based Site Characterization Tools to the Victorville Precision Bombing Range Y and 15 for the ESTCP Wide Area Assessment Demonstration*. PNNL-16138, Pacific Northwest National Laboratory, Richland, Washington. [Unpublished]

Hathaway J, BL Roberts, SA McKenna, and BA Pulsipher. 2007. *Application of Statistically-Based Site Characterization Tools to the Pueblo Precision Bombing and Pattern Gunnery Range #2 for the ESTCP Wide Area Assessment Demonstration*. PNNL-16418, Pacific Northwest National Laboratory, Richland, Washington. [Unpublished]

Hathaway JE, BL Roberts, SA McKenna, and BA Pulsipher. 2008. *Using the VSP-UXO Modules to Support Site Characterization*. PNNL-17382, Pacific Northwest National Laboratory, Richland, Washington. [Unpublished]

National Oceanic and Atmospheric Administration (NOAA). 1962. "NOS Survey H0875, Potomac River." Available at http://surveys.ngdc.noaa.gov/mgg/NOS/GEODAS/h93/H08705_h93.htm.

Roberts BL, J Hathaway, SA McKenna, and BA Pulsipher. 2007. *Application of Statistically-Based Characterization Tools to the Former Erie Army Depot and Toussaint River Site for the ESTCP Wide Area Assessment Demonstration*. PNNL-16550, Pacific Northwest National Laboratory, Richland, Washington. [Unpublished]

United States Army Corps of Engineers (USACE). 2007. Final Site Inspection Report, Aldelphi Laboratory Center – Blossom Point Research Facility Maryland. USACE, Baltimore District, Baltimore Maryland.

Appendix A

Results from Studies Using 500-m and 100-m Window Diameters

Appendix

Results from Studies Using 500-m and 100-m Window Diameters

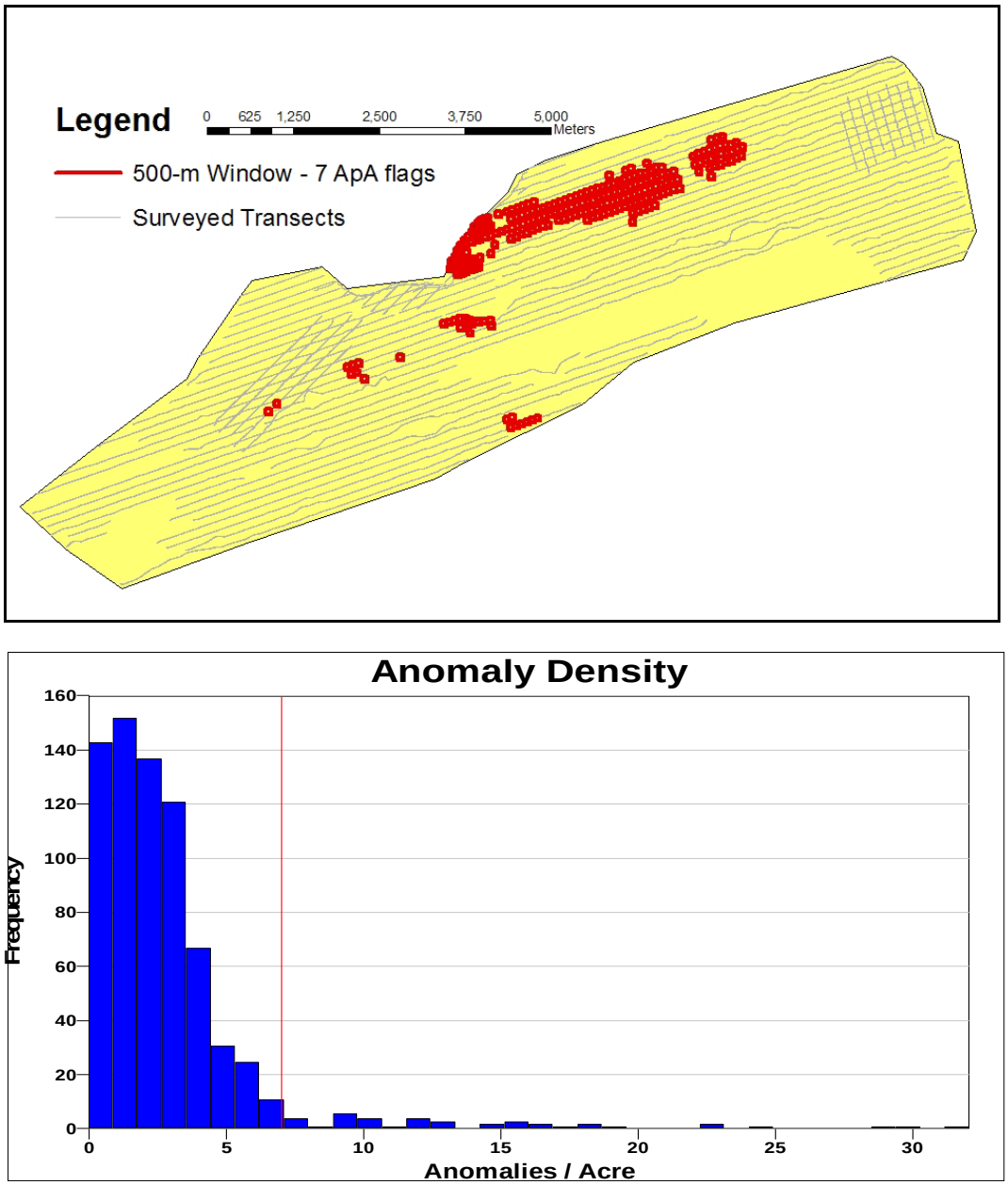

Figure A-1. Flagged high-density regions from a 500-m diameter window using a 7-ApA critical density (top) and the histogram of site densities with a red line marking 7 ApA (bottom).

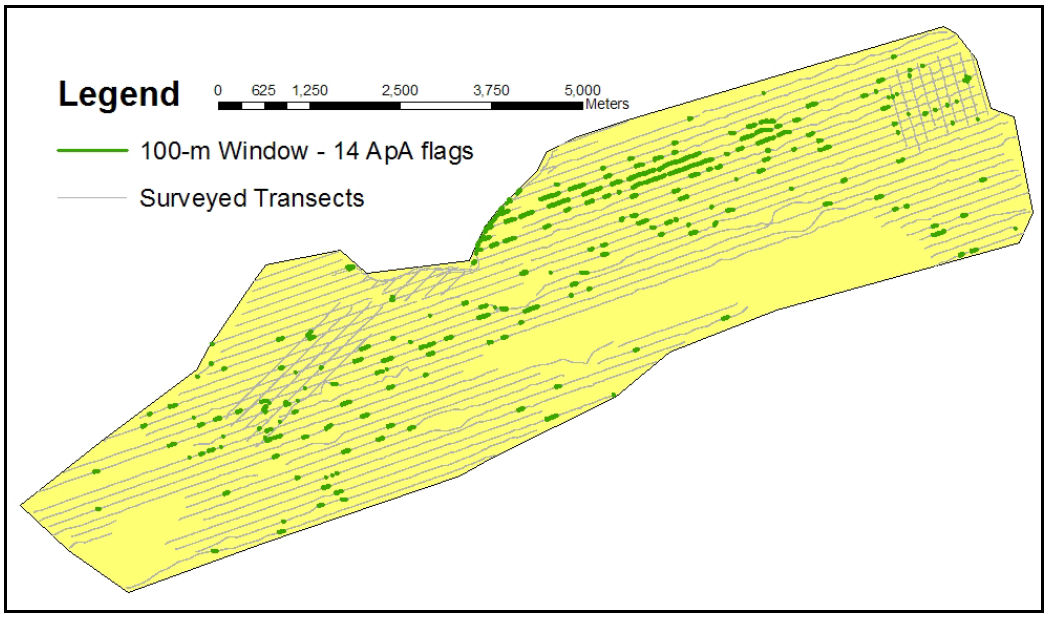

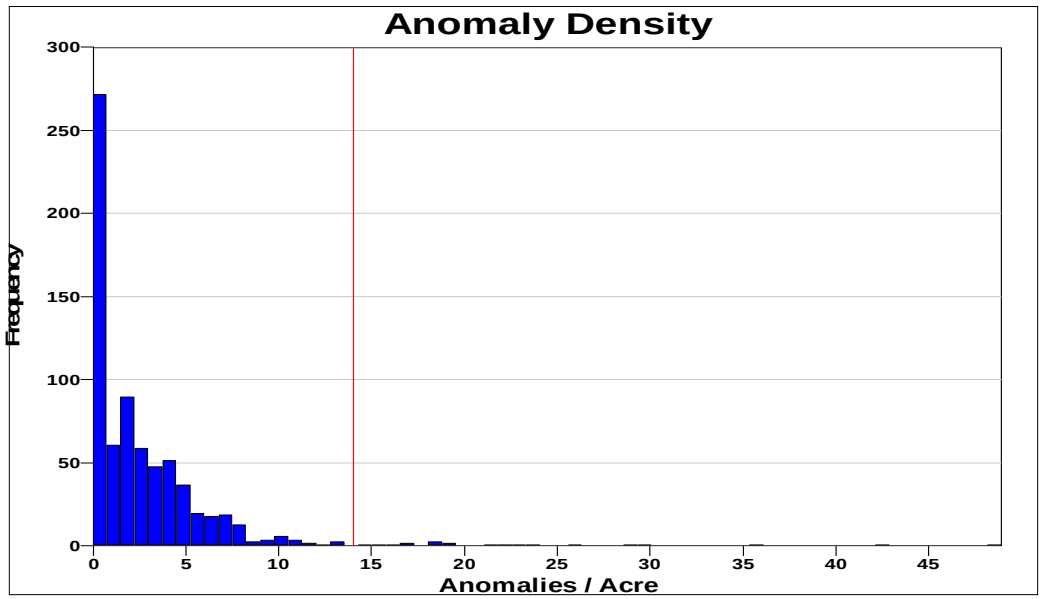

Figure A-2. Flagged high-density regions from a 100-m diameter window using a 14-ApA critical density (top) and the histogram of site densities with a red line marking 14 ApA (bottom).